

## Cu<sup>I</sup> and Ag<sup>I</sup> scorpionate-like complexes based on sterically hindered tris(6-methyl-2-pyridyl)phosphine oxide

Yan V. Demyanov,<sup>a</sup> Irina Yu. Bagryanskaya<sup>b</sup> and Alexander V. Artem'ev<sup>\*a</sup>

<sup>a</sup> A. V. Nikolaev Institute of Inorganic Chemistry, Siberian Branch of the Russian Academy of Sciences, 630090 Novosibirsk, Russian Federation. E-mail: chemisufarm@yandex.ru

<sup>b</sup> N. N. Vorozhtsov Novosibirsk Institute of Organic Chemistry, Siberian Branch of the Russian Academy of Sciences, 630090 Novosibirsk, Russian Federation

DOI: 10.1016/j.mencom.2024.10.014

The interaction of tris(6-methyl-2-pyridyl)phosphine oxide (L) with equimolar amounts of  $[\text{Cu}(\text{MeCN})_4]\text{PF}_6$  or  $\text{AgClO}_4$  in acetonitrile produces scorpionate-like complexes  $[\text{M}(\text{L})(\text{MeCN})]\text{X}$  ( $\text{M} = \text{Cu}$  and  $\text{Ag}$ ;  $\text{X} = \text{PF}_6^-$  and  $\text{ClO}_4^-$ ). At ambient temperature, these compounds exhibit orange ( $\lambda_{\text{max}} = 608 \text{ nm}$ ) or turquoise ( $\lambda_{\text{max}} = 490 \text{ nm}$ ) photoluminescence with a quantum yield up to 16% and lifetimes of microseconds.



**Keywords:** copper(I) and silver(I) complexes, tris(6-methyl-2-pyridyl)phosphine oxide, photoluminescence, crystal structure.

Coinage metal [*i.e.* Cu<sup>I</sup>, Ag<sup>I</sup>, Au<sup>I</sup>] complexes have recently received much research interest by virtue of their applications in materials science,<sup>1–4</sup> catalysis,<sup>5–7</sup> and medicinal chemistry.<sup>8,9</sup> Furthermore, these compounds possess remarkable photophysical properties including thermally activated delayed fluorescence (TADF)<sup>10,11</sup> and efficient room-temperature phosphorescence,<sup>12–14</sup> which promise their as energy-efficient light-emitting devices (PhOLED, pc-LED, LEECs)<sup>1,15–17</sup> and stimuli-responsive materials.<sup>18–21</sup>

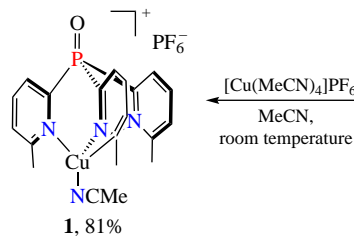
One of the most intriguing class of luminescent coinage metal(I) complexes is represented by so-called ‘scorpionates’ (in which a tridentate ligand binds metal in *fac*-manner). Generally, *N,N',N''*-tripodal ligands, such as tris(pyridyl)methane<sup>22–24</sup> or tris(pyrazolyl)methane and -borate,<sup>25,26</sup> are used for design of Cu<sup>I</sup> and Ag<sup>I</sup> scorpionates. At the same time, other promising tripodal ligands, *e.g.* tris(pyridyl)pnictine chalcogenides, are less investigated in this regard.<sup>27–29</sup>

Herein, we have synthesized a sterically hindered tris(6-methyl-2-pyridyl)phosphine oxide (L) and utilized it as a *N,N',N''*-tripodal ligand for assembly of Cu<sup>I</sup> and Ag<sup>I</sup> scorpionate-

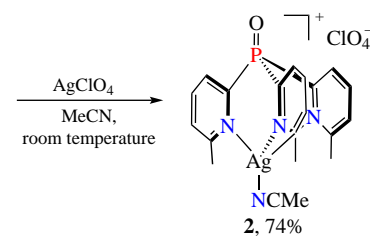
like complexes. The structural and emission properties of the reported compounds are discussed.

We have found that the reaction of  $[\text{Cu}(\text{MeCN})_4]\text{PF}_6$  or  $\text{AgClO}_4$  with 1 equiv. of L readily occurs in MeCN solution at room temperature to afford scorpionate complexes **1** and **2** in 81 and 74% isolated yields, respectively (Scheme 1). The complexes obtained are air and moisture stable powders, well-soluble in MeCN, and marginally soluble in  $\text{CH}_2\text{Cl}_2$ . The powder X-ray diffractometry (XRD) and microanalysis data prove a good phase purity of **1** and **2** (Figures S1 and S2; for details, see Online Supplementary Materials). Their FTIR spectra correlate well with single-crystal XRD and show vibrations from the coordinated phosphine oxide ligands ( $\nu_{\text{C}=\text{C}} = 1488–1447 \text{ cm}^{-1}$ ,  $\nu_{\text{C}=\text{N}} = 1590–1587 \text{ cm}^{-1}$ , and  $\nu_{\text{P}=\text{O}} = 1229–1222 \text{ cm}^{-1}$ ) and MeCN ancillary co-ligands ( $\nu_{\text{C}=\text{N}} = 2273$  and  $2284 \text{ cm}^{-1}$ ). In addition, specific bands of the counterions are observed at  $\nu_{\text{P}=\text{F}} = 843 \text{ cm}^{-1}$  and  $\nu_{\text{Cl}=\text{O}} = 1092 \text{ cm}^{-1}$  (Figures S3 and S4).

Despite the fact that complexes **1** and **2** crystallize in different space groups ( $C2/m$  and  $P\bar{1}$ , respectively),<sup>†</sup> they have quite similar structures (Figure 1). Their cationic parts consist of one



**Scheme 1**



<sup>†</sup> Crystal data for **1**.  $\text{C}_{20}\text{H}_{21}\text{CuF}_6\text{N}_4\text{OP}_2$  ( $M = 572.89$ ), monoclinic, space group  $C2/m$ ,  $a = 17.9479(13)$ ,  $b = 14.5811(8)$  and  $c = 8.8660(6) \text{ \AA}$ ,  $\beta = 92.212(3)^\circ$ ,  $V = 2318.5(3) \text{ \AA}^3$ ,  $Z = 4$ ,  $T = 296 \text{ K}$ ,  $\mu(\text{MoK}\alpha) = 1.150 \text{ mm}^{-1}$ ,  $D_{\text{calc}} = 1.641 \text{ g cm}^{-3}$ . Total of 8084 reflections were measured and 2146 independent reflections ( $R_{\text{int}} = 0.051$ ) were

used in the further refinement. The refinement converged to  $wR_2 = 0.2114$  and  $\text{GOF} = 1.022$  for all independent reflections [ $R_1 = 0.0695$  was calculated against  $F$  for 1761 observed reflections with  $I > 2\sigma(I)$ ].

Crystal data for **2**.  $\text{C}_{20}\text{H}_{21}\text{AgClN}_4\text{O}_5\text{P}$  ( $M = 571.70$ ), triclinic, space group  $P\bar{1}$ ,  $a = 8.7456(6)$ ,  $b = 11.0203(9)$  and  $c = 11.9021(10) \text{ \AA}$ ,

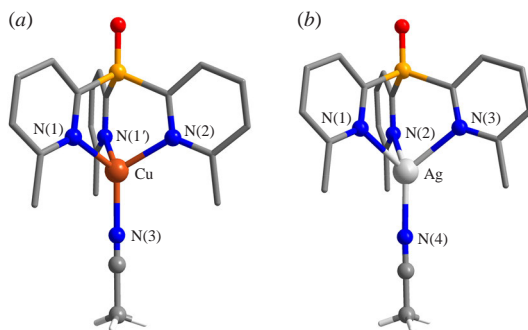


**Figure 1** X-ray derived structures of (a) **1** and (b) **2**. The pyridine H atoms and counterions are not displayed. Selected interatomic distances (Å) and angles (°) for **1**: Cu–N(1) 2.120(4), Cu–N(1') 2.120(4), Cu–N(2) 2.029(7), Cu–N(3) 2.091(5), N(1)–Cu–N(1') 97.6(2), N(2)–Cu–N(1') 118.74(15), N(3)–Cu–N(1') 96.77(15), N(3)–Cu–N(1) 96.77(15), N(2)–Cu–N(1) 118.74(15), N(2)–Cu–N(3) 122.8(3). Symmetry code: (')  $x, 1 - y, z$ . Selected interatomic distances (Å) and angles (°) for **2**: Ag–N(1) 2.166(3), Ag–N(2) 2.331(2), Ag–N(3) 2.379(2), Ag–N(4) 2.350(2), N(3)–Ag–N(4) 128.06(10), N(1)–Ag–N(4) 127.04(10), N(2)–Ag–N(4) 122.61(11), N(1)–Ag–N(3) 89.54(8), N(2)–Ag–N(3) 89.09(8), N(1)–Ag–N(2) 88.40(8).

Cu<sup>I</sup> or Ag<sup>I</sup> ion, which are coordinated by a phosphine oxide ligand in a *N,N',N''*-tripodal manner. The acetonitrile ancillary ligand completes distorted tetrahedral ( $\tau_4 = 0.84$  for **1**) or ‘seesaw’ ( $\tau_4 = 0.74$  for **2**) arrangement of the metal.<sup>30</sup> The distances Cu–N (av. 2.09 Å) and Ag–N (av. 2.31 Å) in **1** and **2** are comparable to the published values.<sup>25,28,29</sup> In the crystal of **1**, PF<sub>6</sub><sup>−</sup> anions are localized between cationic parts and associated with them *via* C<sub>Py</sub>–H···F (2.412 Å) and C<sub>MeCN</sub>–H···F (2.391 and 2.426 Å). Additionally, molecules of **1** are weakly interconnected by  $\pi$ – $\pi$  stacking interactions (C<sub>g</sub>···C<sub>g</sub> ~ 3.815 Å) and C<sub>Py</sub>–H···O (2.544 Å) van der Waals contacts. The packing of **2** contains C<sub>Py</sub>–H···O<sub>L</sub> (2.461 and 2.698 Å), C<sub>MeCN</sub>–H···O<sub>ClO<sub>4</sub></sub> (2.448 Å), and C<sub>Py</sub>–H···C<sub>Py</sub> (2.893 Å) intermolecular contacts. Similar to **1**,  $\pi$ – $\pi$  stacking interactions are observed in crystals of **2** with the mean centroid–centroid distance of 3.798 Å.

The electronic structures in compounds **1** and **2** have been theoretically investigated at a PBE0/def2TZVP level (Figures S5 and S6). The highest occupied molecular orbital (HOMO) and near-HOMOs (HOMO–3 to HOMO–1) of **1** are primarily occupied by the d-orbitals of the Cu atom, while the lowest unoccupied molecular orbitals (LUMO to LUMO+3) consist of  $\pi$ -orbitals on the pyridine rings (Figure S5). Notably, that the HOMO and HOMO–1 of **2** are contributed by d-orbitals of the Ag atom and  $\pi$ -orbitals localized on the pyridine rings. Whereas, the

$\alpha = 102.313(3)^\circ$ ,  $\beta = 90.394(3)^\circ$ ,  $\gamma = 91.284(3)^\circ$ ,  $V = 1120.37(15)$  Å<sup>3</sup>,  $Z = 2$ ,  $T = 200$  K,  $\mu(\text{MoK}\alpha) = 1.130$  mm<sup>−1</sup>,  $D_{\text{calc}} = 1.695$  g cm<sup>−3</sup>. Total of 16651 reflections were measured and 5182 independent reflections ( $R_{\text{int}} = 0.034$ ) were used in the further refinement. The refinement converged to  $wR_2 = 0.0975$  and GOF = 1.048 for all independent reflections [ $R_1 = 0.0375$  was calculated against  $F$  for 4515 observed reflections with  $I > 2\sigma(I)$ ].

The single crystals of **1** were grown by diffusion of hexane vapor into MeCN solution for overnight. Crystals of **2** were obtained by slow evaporation of a MeCN solution overnight. The data were collected on a Bruker Kappa Apex II CCD diffractometer using  $\varphi, \omega$ -scans of narrow (0.5°) frames with MoK $\alpha$  radiation ( $\lambda = 0.71073$  Å) and a graphite monochromator. The structures were solved by direct methods SHELXL97 and refined by a full matrix least-squares anisotropic-isotropic (for H atoms) procedure using the SHELXL-2014/7 program set.<sup>31</sup> Absorption corrections were applied using the empirical multiscan method with the SADABS program.<sup>32</sup> The positions of the hydrogen atoms were calculated with the riding model.

CCDC 2222553 and 2222554 contain the supplementary crystallographic data for this paper. These data can be obtained free of charge from The Cambridge Crystallographic Data Center at <https://www.ccdc.cam.ac.uk>.

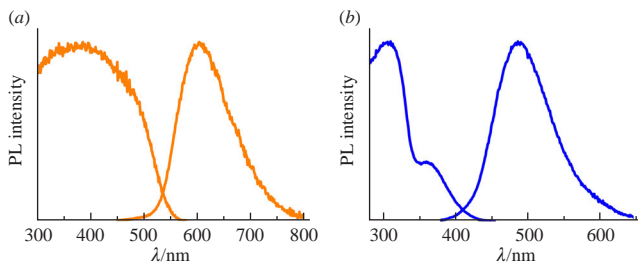


**Figure 2** Emission and excitation spectra of solids (a) **1** and (b) **2** at  $\lambda_{\text{ex}} = 350$  and 300 nm, respectively, at ambient temperature.

HOMO–2 and HOMO–3, as well as LUMO and near-LUMOs, are exclusively presented by pyridine  $\pi$ -orbitals (Figure S6). The orbitals on MeCN co-ligands make almost no contribution to the frontier orbitals of complexes **1** and **2**. Thus, the low-energy excited states of **1** and **2** should have a (metal + ligand)-to-ligand charge transfer character, *i.e.*, (M+L)LCT.

We have also investigated the luminescent properties of **1** and **2** in the solid state. Upon UV illumination at ambient temperature, both complexes exhibit moderate orange (**1**) or turquoise (**2**) luminescence, respectively. The emission spectra of **1** and **2** display broad bands maximized at 608 and 490 nm, respectively (Figure 2). Note that the emission maxima are independent of the excitation wavelength. The emission lifetimes of 5.5 and 11.2  $\mu$ s for **1** and **2** at 298 K suggest that the observed luminescence originated from phosphorescence or TADF. The photoluminescence quantum yields (298 K) for **1** and **2** are 16% and 6%, respectively. Considering these facts and the results of our DFT calculations, the emission can probably be ascribed to phosphorescence or TADF of (M+L)LCT, which is often observed for Cu<sup>I</sup> and Ag<sup>I</sup> complexes.<sup>1,2,10–12,28,29</sup>

In conclusion, a pair of new scorpionate-like complexes [M(L)(MeCN)]X (M = Cu and Ag; X = PF<sub>6</sub><sup>−</sup> and ClO<sub>4</sub><sup>−</sup>) based on tris(6-methyl-2-pyridyl)phosphine oxide (L) has been synthesized. At ambient temperature, these complexes demonstrate bright orange (M = Cu; X = PF<sub>6</sub><sup>−</sup>) or turquoise (M = Ag; X = ClO<sub>4</sub><sup>−</sup>) solid-state photoluminescence. The results obtained provide a new understanding of coordination chemistry of *N,N',N''*-tripodal ligands, and also contribute to photophysics of coinage metal(I) complexes.

This work was supported by the Ministry of Science and Higher Education of the Russian Federation (projects nos. 121031700321-3, 121031700313-8 and 1021051503141-0-595-1.4.1). The authors are grateful to Dr. M. I. Rakhmanova (NIIC SB RAS) for recording emission and excitation spectra of **1** and **2**, and to Dr. E. H. Sadykov (NIIC SB RAS) for running DFT computations.

#### Online Supplementary Materials

Supplementary data associated with this article can be found in the online version at doi: 10.1016/j.mencom.2024.10.014.

#### References

- 1 V. W.-W. Yam, V. K.-M. Au and S. Y.-L. Leung, *Chem. Rev.*, 2015, **115**, 7589; <https://doi.org/10.1021/acs.chemrev.5b00074>.
- 2 E. Cariati, E. Lucenti, C. Botta, U. Giovanella, D. Marinotto and S. Righetto, *Coord. Chem. Rev.*, 2016, **306**, 566; <https://doi.org/10.1016/j.ccr.2015.03.004>.
- 3 V. K.-M. Au, *Energy Fuels*, 2021, **35**, 18982; <https://doi.org/10.1021/acs.energyfuels.1c01956>.
- 4 C. Lescop, *Chem. Rec.*, 2021, **21**, 544; <https://doi.org/10.1002/tcr.202000144>.
- 5 S. Hanf, R. García-Rodríguez, A. D. Bond, E. Hey-Hawkins and D. S. Wright, *Dalton Trans.*, 2016, **45**, 276; <https://doi.org/10.1039/C5DT04155D>.

6 M. K. Rong, F. Holtrop, J. C. Slootweg and K. Lammertsma, *Coord. Chem. Rev.*, 2019, **380**, 1; <https://doi.org/10.1016/j.ccr.2018.08.016>.

7 T.-H. Chiu, J.-H. Liao, R. P. Brocha Silalahi, M. N. Pillay and C. W. Liu, *Nanoscale Horiz.*, 2024, **9**, 675; <https://doi.org/10.1039/D4NH00036F>.

8 M. Marinelli, C. Santini and M. Pellei, *Curr. Top. Med. Chem.*, 2016, **16**, 2995; <https://doi.org/10.2174/1568026616666160506145408>.

9 A. Tialiou, J. Chin, B. K. Keppler and M. R. Reithofer, *Biomedicines*, 2022, **10**, 1417; <https://doi.org/10.3390/biomedicines10061417>.

10 R. Czerwieniec, M. J. Leitl, H. H. H. Homeier and H. Yersin, *Coord. Chem. Rev.*, 2016, **325**, 2; <https://doi.org/10.1016/j.ccr.2016.06.016>.

11 Ya. V. Demyanov, M. I. Rakhmanova, I. Yu. Bagryanskaya and A. V. Artem'ev, *Mendeleev Commun.*, 2022, **32**, 649; <https://doi.org/10.1016/j.mencom.2022.09.027>.

12 A. A. Titov, O. A. Filippov, A. F. Smol'yakov, A. A. Averin and E. S. Shubina, *Mendeleev Commun.*, 2021, **31**, 170; <https://doi.org/10.1016/j.mencom.2021.03.008>.

13 Ya. V. Demyanov, M. I. Rakhmanova, I. Yu. Bagryanskaya and A. V. Artem'ev, *Mendeleev Commun.*, 2023, **33**, 484; <https://doi.org/10.1016/j.mencom.2023.06.014>.

14 R. M. Khisamov, A. A. Ryadun, S. N. Konchenko and T. S. Sukhikh, *Molecules*, 2022, **27**, 8162; <https://doi.org/10.3390/molecules27238162>.

15 O. S. Wenger, *Chem. Rev.*, 2013, **113**, 3686; <https://doi.org/10.1021/cr300396p>.

16 Y. Wang, Y. Shi, X. Zou, Y. Hea and X. Wang, *CrystEngComm*, 2019, **21**, 5595; <https://doi.org/10.1039/C9CE00943D>.

17 C.-Y. Liu, X.-R. Chen, H.-X. Chen, Z. Niu, H. Hirao, P. Braunstein and J.-P. Lang, *J. Am. Chem. Soc.*, 2020, **142**, 6690; <https://doi.org/10.1021/jacs.0c00368>.

18 W. Liu, Y. Fang, G. Z. Wei, S. J. Teat, K. Xiong, Z. Hu, W. P. Lustig and J. Li, *J. Am. Chem. Soc.*, 2015, **137**, 9400; <https://doi.org/10.1021/jacs.5b04840>.

19 M.-C. Tang, A. K.-W. Chan, M.-Y. Chan and V. W.-W. Yam, *Top. Curr. Chem.*, 2016, **374**, 46; <https://doi.org/10.1007/s41061-016-0046-y>.

20 C. E. Housecroft and E. C. Constable, *J. Mater. Chem. C*, 2022, **10**, 4456; <https://doi.org/10.1039/D1TC04028F>.

21 A. Schlachter, F. Moutier, R. Utrera-Melero, J. Schiller, A. M. Khalil, G. Calvez, M. Scheer, K. Costuas and C. Lescop, *Adv. Opt. Mater.*, 2024, **12**, 2400347; <https://doi.org/10.1002/adom.202400347>.

22 C. S. Letko, T. B. Rauchfuss, X. Zhou and D. L. Gray, *Inorg. Chem.*, 2012, **51**, 4511; <https://doi.org/10.1021/ic202207e>.

23 T. Gneuß, M. J. Leitl, L. H. Finger, H. Yersin and J. Sundermeyer, *Dalton Trans.*, 2015, **44**, 20045; <https://doi.org/10.1039/C5DT03065J>.

24 A. Schinabeck, N. Rau, M. Klein, J. Sundermeyer and H. Yersin, *Dalton Trans.*, 2018, **47**, 17067; <https://doi.org/10.1039/C8DT04093A>.

25 G. G. Lobbia, J. V. Hanna, M. Pellei, C. Pettinari, C. Santini, B. W. Skelton and A. H. White, *Dalton Trans.*, 2004, 951; <https://doi.org/10.1039/B316815H>.

26 S. G. Ridlen, N. V. Kulkarni and H. V. R. Dias, *Polyhedron*, 2017, **125**, 68; <https://doi.org/10.1016/j.poly.2016.09.014>.

27 T. Gneuß, M. J. Leitl, L. H. Finger, N. Rau, H. Yersin and J. Sundermeyer, *Dalton Trans.*, 2015, **44**, 8506; <https://doi.org/10.1039/C4DT02631D>.

28 A. J. Plajer, D. Crusius, R. B. Jethwa, Á. García-Romero, A. D. Bond, R. García-Rodríguez and D. S. Wright, *Dalton Trans.*, 2020, **50**, 2393; <https://doi.org/10.1039/D0DT03732J>.

29 A. V. Artem'ev, J. A. Eremina, E. V. Lider, O. V. Antonova, E. V. Vorontsova and I. Yu. Bagryanskaya, *Polyhedron*, 2017, **138**, 218; <https://doi.org/10.1016/j.poly.2017.09.041>.

30 L. Yang, D. R. Powell and R. P. Houser, *Dalton Trans.*, 2007, 955; <https://doi.org/10.1039/B617136B>.

31 G. M. Sheldrick, *Acta Crystallogr.*, 2015, **A71**, 3; <https://doi.org/10.1107/S2053273314026370>.

32 *Bruker Apex3 Software Suite: Apex3, SADABS-2016/2 and SAINT*, version 2018.7-2, Bruker AXS, Madison, WI, 2017.

Received: 21st June 2024; Com. 24/7549